Fig. 5. Interval of bedded lacustrine strata shown in measured section M-6 (Fig. 4); beds are overlain by cliff-forming bomb-rich unit.

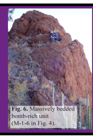

Fig. 6. Massively bedded bomb-rich unit (M-1-6 in Fig. 4).

Intrusive pyroclastic rocks formed during explosive andesitic eruptions in a Mesoproterozoic volcanic arc setting, Barby Formation, SW Namibia

Sierra Ohrmundt (sierra.ohrmundt@tcu.edu), Richard E. Hanson, and Virginia Andrews
School of Geology, Energy, and the Enviornment, Texas Christian University, Fort Worth

Fig. 7. Basaltic andesite bombs in lapillistone matrix (unit M-7-3 in Fig. 4).

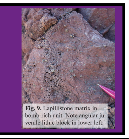

Fig. 9. Lapillistone matrix in bomb-rich unit. Note angular juvenile lithic block in lower left.

Abstract

Mesoproterozoic volcanic arc rocks in the Barby Formation are extensively exposed in mountainous desert terrain in SW Namibia. Here we report results of detailed mapping of a representative succession of pyroclastic fall deposits intercalated with lacustrine strata consisting mostly of planar-bedded mudstone, siltstone and sandstone. Individual pyroclastic fall deposits are up to ~80 m thick and contain various amounts of fluidal to angular lapilli intermixed with ellipsoidal bombs up to 60 cm across, indicating deposition close to source vents that were primarily undergoing Strombolian-style eruptions.

Also present are enigmatic pyroclastic rocks (basaltic andesite in composition) that intrude lacustrine sedimentary packages at a number of locations spread out laterally for ~600 m over a vertical stratigraphic distance of ~300 m. The intrusive pyroclastic rocks consist of moderately to highly vesicular lapilli and dispersed, less vesicular bombs and are lithologically similar to some of the extrusive pyroclastic units. In one area the pyroclastic material forms a 1-m-wide dike intruded into lacustrine strata. More commonly the pyroclastic intrusions form structureless masses ≥ 12 m across that transgress bedding in the lacustrine sequences and in places enclose rafts of sediment that have been rotated relative to intact strata nearby. The sediment rafts show varying degrees of disruption and local peperitic mixing with intrusive pyroclastic material. How these pyroclastic intrusions were emplaced is unclear. Possibly they represent pyroclastic jets injected laterally into weak layers of unconsolidated, fine-grained sediment from vent conduits that fed explosive eruptions at higher levels (not exposed); we plan to test this hypothesis during future field work.

In most cases, zones of peperite up to 3 m thick separate the pyroclastic intrusions from host lacustrine sequences and consist of abundant fluidal bodies of vesicular basaltic andesite up to 50 cm across mingled with fine-grained sediment preserving planar lamination to various degrees. We infer that these peperites formed after explosive activity had ceased, when small batches of magma preferentially intruded along zones of weakness between the intrusive pyroclastic material and adjacent sediment.

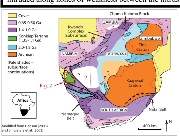

Fig. 1. Location of the Konkiep terrane within the Precambrian tectonic framework of southern Africa.

Introduction

Well-preserved 1.2 Ga volcanic arc rocks exposed in rugged desert country in SW Namibia provide cross-sectional views of a stratigraphically thick and complex array of lavas, pyroclastic deposits, intercalated lacustrine units, feeder conduits to volcanic vents, and associated hypabyssal magma plumbing networks. None of these rocks have previously been studied in any detail from a modern volcanological perspective. Here we describe an unusual series of intrusive pyroclastic rocks and associated peperites of basaltic andesite composition that were injected into unlithified strata at shallow levels beneath the surface.

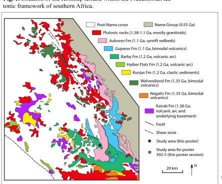

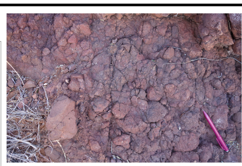

Fig. 9. Lapillistone matrix in bomb-rich unit. Note angular juvenile lithic block in lower left.

Fig. 2. Geological map of the main part of the Konkiep terrane, showing location of study areas for this poster and poster 392-5 (this poster session) by Andrews et al.

Geologic Framework

Mesoproterozoic arc rocks in SW Namibia occur within the Konkiep terrane (Fig. 1), which is a major tectonic element within the 1.4-1.0 Ga Namaqua-Natal orogenic belt that extends along the southern margin of the Archean Kaapvaal craton and represents one of the main convergent margins active during assembly of the Rodinia supercontinent (Hanson 2003; Jacobs et al., 2008; Miller, 2012). The Konkiep terrane contains a series of volcanic and clastic sedimentary units and associated, dominantly granitoid plutonic rocks separated partly by major unconformities (Fig. 2; Watters, 1974; Miller, 2008). Metamorphic grade is typically in the zeolite and prehnite-pumpellyite facies. The timing of the different magmatic events recorded in the terrane is constrained primarily by U-Pb zircon crystallization ages (Miller, 2008; Cornell et al., 2015, 2016; Panzik et al., 2016). These data show that island-arc tholeiitic rocks of the ~1.38 Ga Kairab Formation represent the earliest arc magmatism in the terrane. Following accretion of this arc and its underlying metamorphic basement, renewed magmatism at ~1.35 Ga formed the bimodal (basaltic and rhyolitic) Nagatis and Welverdiend Formations, probably in rift environments. Development of a new continental margin arc is recorded by the ~1.2 Ga calc-alkaline Haiber Flats Formation and the calc-alkaline to shoshonitic Barby Formation, which is located farther inboard (Watters, 1974; Brown and Wilson, 1986; Hoal, 1990; Miller, 2012). These rocks are unconformably overlain by 1.1 Ga synrift bimodal rocks of the Guperas Formation and slightly younger redbeds of the Aubores Formation (Miller, 2008; Panzik et al., 2016).

The Barby Formation, which is the focus of the present work, contains a composite volcanic arc stratigraphic succession as much as 12 km thick. Our recent mapping in two well-exposed areas (Fig. 2) has revealed that significant parts of the formation consist of Hawaiian, Strombolian and phreatomagmatic pyroclastic deposits that were emplaced close to source vents (fissures or scoria and spatter cones) and are intercalated with fine-grained lacustrine strata, which are ubiquitous throughout the study area. The facies relations are consistent with the interpretation that these rocks accumulated in extensional basins during oblique subduction along the convergent margin (Hoal, 1993). At least in the limited areas we have so far investigated, there is no evidence for high-standing stratovolcanoes.

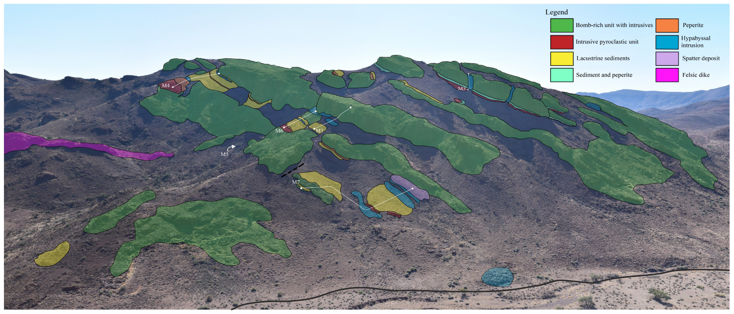

Fig. 3. Oblique cross-sectional view of the study area, looking east. Locations of measured sections in Fig. 4 are indicated.

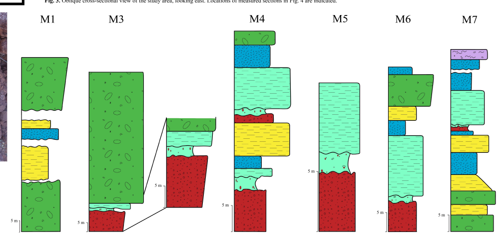

Fig. 4. Representative measured sections; locations are shown in Fig 3.

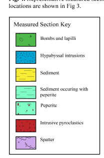

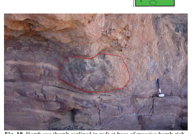

Fig. 10. Bomb sag (bomb outlined in red) at base of massive bomb-rich unit overlying lacustrine strata.

Fig. 11. Angular, poorly vesicular lapilli within a pocket of lapilli tuff that grades into more common lapillistone matrix (not visible in this view) in a bomb-rich unit.

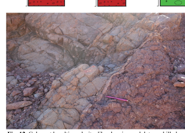

Fig. 12. Coherent basaltic andesite dike showing undulatory chilled margin against intrusive pyroclastic rock to right.

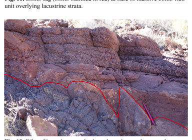

Fig. 13. Dike of intrusive pyroclastic rock cutting sandstone and granule conglomerate. View is perpendicular to dike wall; pencil lies on host sediment behind dike. Margin of dike is outlined.

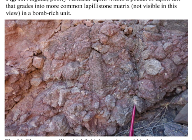

Fig. 14. Elongate to ellipsoidal fluidal pyroclasts within intrusive pyroclastic rock (unit M-3-1 in Fig. 4).

Fig. 15. Large mass of peperite intruding bedded sediment beneath a massive, bomb-rich unit. Fluidal basaltic andesite clasts in peperite weather more readily than the sediment host (examples are labeled "ba"). Arrow points to truncation of bedding in overlying sediment against discordant contact with peperite.

Fig. 16. Closer view of area indicated by arrow in Fig. 15.

Study Area

The study area for this poster is located on the western margin of a half-graben occupied by post-Barby redbeds of the Aubores Formation (Fig. 2). Results of similar work on the other side of the half-graben are presented in Poster 392-5 in this session by Andrews et al. Figure 3 is an oblique view of most of the study area and illustrates the main extrusive and intrusive lithofacies present, discussed below. Figure 4 shows representative measured sections of some of the units. The various units contain similar phenocryst populations (augite and altered olivine), suggesting they are closely linked petrogenetically. Groundmass textures typically range from tachylitic to intersertal and intergranular. Based on petrographic comparisons with samples from other parts of the Barby Formation for which we have geochemical analyses (Andrews and Hanson, unpubl. data), we infer that the extrusive and intrusive rocks in the present study area are basaltic andesite to shoshonite in composition; geochemical studies of these rocks are in progress.

Lacustrine Deposits

The main extrusive pyroclastic deposits in the study area are separated by sequences up to 20 m thick of dominantly planar-bedded andesitic volcaniclastic mudstone, siltstone, sandstone and granule conglomerate (Figs. 4 and 5) inferred to have been deposited by sediment gravity flows and suspension sedimentation in lacustrine settings. Delicate planar lamination is characteristic of the finer grained clastic rocks, and coarser debris-flow and turbidite deposits typically form tabular units that are laterally continuous on the scale of individual outcrops.

Pyroclastic Deposits

The most impressive pyroclastic deposits are cliff-forming, poorly sorted, bomb-rich units as much as 80 m thick with little evidence of internal layering (Figs. 6 and 7). These units contain variable amounts of fluidal, elongate to ellipsoidal bombs ≤ 60 cm across, in which vesicularity ranges from 10 to 50 %, based on visual estimates. Pieces of spatter (Fig. 8) and juvenile angular lithic clasts up to 15 cm across (Fig. 9) occur in smaller amounts. Bomb sags are well developed where the bomb-rich deposits rest directly on lacustrine beds (Fig. 10). Agglomerate is present locally where the bombs are closely packed, but they are generally dispersed within a matrix consisting dominantly of lapillistone (Figs. 7 and 9). Individual lapilli most commonly have fluidal outlines with ovoid, droplet-like, or somewhat elongate shapes and show the same range in vesicularity as the bomb (Fig. 9). Beds of coalesced spatter also occur (Fig. 4, measured section 7). These characteristics and the features exhibited by the bombs indicate derivation from explosive eruptions showing transitional Strombolian to Hawaiian behavior.

The lapillistone in some cases grades into meter-scale pockets of lapilli tuff that contain angular, blocky, poorly vesicular ash- and lapilli-sized particles (Fig. 11). In some cases, partly disaggregated pieces of sand and mud ≤ 60 cm long also occur within the lapilli tuff. Based on these features, we interpret the lapilli tuff to record a phreatomagmatic component in some of the eruptions, involving explosive interactions between basaltic andesite magma and water-rich lake sediment.

Intrusive Pyroclastic Rocks

We have found pyroclastic rocks that show clear intrusive relations with lacustrine strata at 12 separate locations within the study area over a lateral distance of ~600 m and a vertical stratigraphic distance of ~300 m. The intrusive pyroclastic rocks form massive bodies ≥ 12 m across (Fig. 12), but their full dimensions are generally unclear because some of their margins covered. They transgress bedding in the lacustrine sediments, and in one case form a 1-m-dike injected into the host sediments (Fig. 13). Tabular masses of sandstone up to 3 m long are enclosed within the pyroclastic material and show partly disrupted bedding and mixing along their margins with the adjacent pyroclasts. The intrusive pyroclastic rocks contain the same types of bombs dispersed in lapillistone or lapilli tuff as seen in the extrusive pyroclastic deposits (Figs. 12 and 14). The bombs tend to be smaller (≤ 20 cm) than in the extrusive deposits, but otherwise the pyroclasts in the intrusive and extrusive units are indistinguishable. An intrusive origin is only obvious when the contacts of these pyroclastic masses with the adjacent host sedimentary strata are exposed.

Peperite

In most cases, zones of peperite up to 10 m thick separate the intrusive pyroclastic rocks from the overlying host sedimentary strata (Figs. 4 and 15), and in places the peperite shows discordant contacts against relatively undisturbed bedded lacustrine deposits (Figs. 15 and 16). The peperite consists of fluidal clasts of basaltic andesite ≤ 50 cm across that contain 30-40 % vesicles and are surrounded by partly disrupted sandstone, siltstone and mudstone, in which planar lamination is preserved to various degrees (Fig. 17).

Coherent Hypabyssal Intrusions

Coherent intrusions of poorly to nonvesicular basaltic andesite are common throughout the study area. They consist of dikes ≤ 10 m wide, sills ≤ 7 m thick and discordant intrusions with more irregular shapes as much as 50 m across. The dikes typically have planar chilled margins where they crosscut cliff-forming, bomb-rich units, but these margins become undulatory where the dikes intrude lacustrine strata, intrusive pyroclastic rocks and peperite (Fig. 12). In places, elongate, branching intrusive tongues up to several meters long extend from dikes or irregular intrusions into the adjacent units. Some of the tongues show partial disaggregation where they penetrated pyroclastic material (Fig. 18).

Fig. 17. View of peperite from a different area, showing fluidal bodies of vesicular basaltic andesite (outlined) separated by disrupted sediment that partly preserves planar lamination.

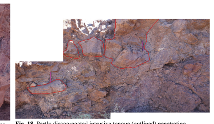

Fig. 18. Partly disaggregated intrusive tongue (outlined) penetrating extrusive pyroclastic deposits

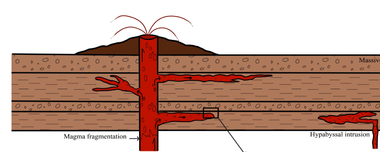

Fig. 19. Model for formation of intrusive pyroclastic rocks (see Interpretation section of poster for explanation).

Interpretation

Features shown by the prominent, bomb-rich units in the study area indicate that they accumulated close to source vents undergoing Hawaiian and Strombolian eruptions, with some phreatomagmatic input at times. Bomb sags are present in all cases where the deposits rest directly on lacustrine strata (Fig. 9), which must have been unlithified and moist (cohesive) when the bombs impacted. However, the pyroclasts show no evidence of rapid aqueous chilling or nonexplosive quench fragmentation of the type that would be expected if they fell into lakes containing a significant amount of water. The lakes were probably shallow at any given time, so that rapid influx of coarse pyroclasts dominated the thermal regime and suppressed aqueous quenching.

Additional evidence that the lacustrine sediments were wet and unconsolidated during the volcanic activity is provided by peperitic interactions between intrusive magma and sediment, and by the presence of partly disaggregated sediment masses contained within intrusive pyroclastic rocks. We infer that intercalation of massive bomb-rich units with generally fine-grained, unconsolidated sediments rich in pore water created a setting favorable for intrusive pyroclastic activity. A model for the development of the intrusive pyroclastic rocks is shown in Fig. 19, in which a postulated vent conduit feeding explosive pyroclastic eruptions at the surface is shown cutting across previously deposited pyroclastic and lacustrine units. We infer that, at times during the ongoing eruption, jets of intrusive pyroclastic material were blasted laterally from the conduit into layers of mechanically weak sediments forming parts of the conduit walls. This might have been triggered when collapse of parts of the ejecta rim or walls into the conduit at higher levels impeded upwards thrust of gas and pyroclasts from magmatic explosions originating deeper in the conduit. Several examples of the intrusive pyroclastic rock occur only a short distance below the massive, bomb-rich pyroclastic units (e.g., measured section M-3 in Fig. 4), suggesting that these units resisted penetration by the intrusive pyroclastic material, resulting in significant lateral motion of the pyroclastic jets into weak sediments between bomb-rich layers. Liquefaction and fluidization of the sediments as their pore water was converted to steam likely helped create space for the intrusive pyroclastic jets.

Zones of peperite must have formed after explosive activity ceased, when magma rising up in the conduit intruded along planes of weakness between still unconsolidated, water-rich sediment and intrusive pyroclastic material (Fig. 19). Nonexplosive quenching and commingling of the intruding magma with wet sediment created intricate small-scale intrusive geometries (Figs. 15-17). Coherent hypabyssal intrusions in the area also were injected into unconsolidated material, as shown by the common presence of undulatory chilled margins along intrusive contacts (cf., Keating et al., 2008; Befus et al., 2009) and by breakup of some intrusive tongues penetrating intrusive pyroclastic bodies (Figs. 12 and 18).

Reports of intrusive pyroclastic rocks in the literature are relatively sparse, although several examples have been described of welded felsic ignimbrites filling vents that supplied explosive magmatic eruptions (Wolff, 1986; Reedman et al., 1987). Tuffisite injections in felsic and andesitic lava flows and domes appear to be common (e.g., Tuffen et al., 2003) but are developed on a much smaller scale. Dikes and sills filled with pyroclasts generated during subsurface phreatomagmatic explosions have also been reported (e.g., Hanson and Elliot, 1996). Reports of intrusive basaltic to andesitic pyroclastic rocks of the type described in the present poster, consisting of vesicular lapilli and bombs, are much less common. One well documented Miocene example in California consists of a complex of sills and dikes that extends laterally for ~10 km and formed when intrusive andesitic pyroclasts (pumice lapilli and ash) were injected into unlithified diatomite at very shallow levels beneath the seafloor (Schleicher, 1974).

It is possible that intrusive basaltic to andesitic pyroclastic rocks are more common than generally realized but have been overlooked because they closely resemble extrusive pyroclastic deposits produced by Hawaiian or Strombolian eruptions. Detailed studies in other volcanic terrains that expose hypabyssal magma plumbing systems together with associated extrusive pyroclastic deposits or volcanic vents are likely to reveal other examples.

References

Befus, K.S., Hanson, R.E., Miggins, D.P., Breyer, J.A., and Busbey, A.B., Nonexplosive and explosive magma/wet-sediment interaction during emplacement of Eocene intrusions into Cretaceous to Eocene strata, Trans-Pecos igneous province, West Texas: Journal of Volcanology and Geothermal Research, v. 181, p. 155-172.
Brown, G.J., and Wilson, A.H., 1986, The petrology and geochemistry of the Barby Formation, Sinclair Sequence: Communications of the Geological Survey of Southwest Africa/Namibia, v. 2, p. 93-108.
Cornell, D.H., van Schijndel, V., Simonsen, S.L., and Frei, D., 2015, Geochronology of Mesoproterozoic hybrid intrusions in the Konkiep terrane, Namibia, from passive to active continental margin in the Namaqua-Natal Wilson cycle: Precambrian Research, v. 265, p. 166-188.
Cornell, D.H., Mapani, B., Malobela, T., Lundell, C., Harris, M., Jonsson, A., and Frei, D., 2016, Precise zircon dating identifies the threefold evolution of the Sinclair Supergroup of Namibia: Abstracts, 35th International Geological Congress, Capetown, South Africa.
Hanson, R.E., 2003, Proterozoic geochronology and tectonic evolution of southern Africa, in Yoshida, M., Windley, B., and Dasgupta, S., eds., Proterozoic East Gondwana: Supercontinent Assembly and Breakup: Geological Society of London Special Publication 206, p. 428-463.
Hanson, R.E., and Elliot, D.H., Rift-related Jurassic basaltic phreatomagmatism in the central Transantarctic Mountains: precursory stage to flood-basalt volcanism: Bulletin of Volcanology, v. 58, p. 327-347.
Hoal, B.G., 1990, The geology and geochemistry of the Proterozoic Awasib Mountain Terrain, southern Namibia: Geological Survey of Namibia, Memoir 11, 163 p.
Hoal, B.G., 1993, The Proterozoic Sinclair Sequence in southern Namibia: intracratonic rift or active continental margin setting? Precambrian Research, v. 63, p. 143-162.
Jacobs, J., Pisarevsky, S., Thomas, R.J., and Becker, T., 2008, The Kalahari craton during the assembly and dispersal of Rodinia: Precambrian Research, v. 160, p. 142-158.
Keating, G.N., Valentine, G.A., Krier, D.J., and Perry, F.V., 2008, Shallow plumbing systems for small-volume basaltic volcanoes: Bulletin of Volcanology, v. 709, p. 563-582.
Miller, R.McG., 2008, The Geology of Namibia, Vol. 1, Archaean to Mesoproterozoic: Windhoek, Geological Survey of Namibia, p. 8-1 to 8-104.
Miller, R.McG., 2012, Review of Mesoproterozoic magmatism, sedimentation and terrane amalgamation in southwestern Africa: South African Journal of Geology, v. 115, p. 417-448.
Panzik, J.E., Evans, D.A.D., Kasbohm, J.J., Hanson, R., Gose, W., and DesOrmeau, J., 2016, Using palaeomagnetism to determine late Mesoproterozoic palaeogeographic history and tectonic relations of the Sinclair Terrane, Namaqua orogen, Namibia, in Li, Z.X., Evans, D.A.D., and Murphy, J.B., eds., Supercontinent Cycles through Earth History: Geological Society of London Special Publication 424, p. 119-143.
Reedman, A.J., Park, K.H., Merriman, R.J., and Kim, S.E., 1987, Welded tuff infilling a volcanic vent at Weolseong, Republic of Korea: Bulletin of Volcanology, v. 49, p. 541-546.
Schleicher, D., 1974, Emplacement mechanism of the Miraleste Tuff Bed, Palos Verdes Hills, California: Geological Society of America Bulletin, v. 85, p. 505-512.
Tuffen, H., Dingwell, D.B., and Pinkerton, H., 2003, Repeated fracture and healing of silicic magma generate flow banding and earthquakes? Geology, v. 31, p. 1089-1992.
Watters, B.R., 1974, Stratigraphy, igneous petrology and evolution of the Sinclair Group in southern South West Africa: University of Cape Town, Precambrian Research Unit Bulletin 16, 235 p.
Wolff, J.A., 1986, Welded-tuff dykes, conduit closure, and lava dome growth at the end of explosive eruptions: Journal of Volcanology and Geothermal Research, v. 28, p. 379-384.